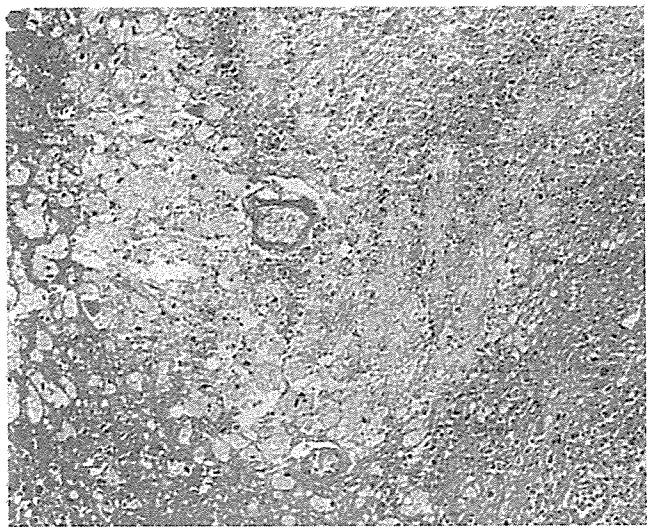

Fig. 5. Microscopic findings obtained from case 3. Lower-power view showing hyalinized tissue and reactive glia, H and E.

cal characteristics such as cellularity, vascularity and/or fiber structure, and this correlation thereby leads to a tendency for tumors of higher grade to present with higher FA values [12,13,16].

The relationship between the FA value and each histological type of astrocytic tumors has been reported, with mean FA values of 0.24 ± 0.06 in glioblastoma, 0.19 ± 0.06 in anaplastic astrocytomas, 0.12 ± 0.02 in diffuse astrocytomas and 0.16 ± 0.02 in pilocytic astrocytomas [12]. A relationship between FA value and the WHO classification of gliomas has also been reported. The FA value of grade 1 gliomas (0.150 ± 0.017) is significantly lower than that of grade 3 (0.23 ± 0.033) or grade 4 (0.229 ± 0.033) gliomas. The FA value of grade 2 gliomas (0.159 ± 0.018) is significantly lower than those of grade 3 or 4 gliomas [16]. In our cases, the FA values of recurrent tumor were 0.27 ± 0.04 and 0.29 ± 0.04, which are equivalent to the previously reported FA value of primary gliomas. These two cases were diagnosed as tumor recurrence by histopathological examination. The FA value of case 3 revealed a low value in the enhanced lesion. This case was diagnosed as radiation necrosis by histopathological examination. In radiation necrosis tissue, there are no normal fibers or cell structures, and thus the directionality of water diffusion is decreased. Consequently, the FA value of radiation necrosis tissue may be lower than that of tumor recurrence (Fig. 5).

In conclusion, although our observations were limited to only three cases, they suggest that the assessment of FA value in enhanced lesions after radiotherapy may be able to differentiate radiation necrosis from tumor recurrence. This non-invasive technique will most likely become an option for auxiliary examinations for histological diagnosis after adjuvant radiotherapy. Using FA value, unnecessary craniotomies may be avoided in the future.

Acknowledgments

This work was supported in part by Grants-in-Aid for Advanced Medical Science Research by the Ministry of Education, Culture, Sports, Science, and Technology, Japan.

References

[1] Covarrubias DJ, Rosen BR, Lev MH. Dynamic magnetic resonance perfusion imaging of brain tumors. Oncologist 2004;9:528–37.

[2] Patronas NJ, Di Chiro G, Brooks RA, DeLaPaz RL, Kornblith PL, Smith BH, et al. Work in progress: [^{18}F] fluorodeoxyglucose and positron emission tomography in the evaluation of radiation necrosis of the brain. Radiology 1982;144:885–9.

[3] Tsuyuguchi N, Sunada I, Iwai Y, Yamanaka K, Tanaka K, Takami T, et al. Methionine positron emission tomography of recurrent metastatic brain tumor and radiation necrosis after stereotactic radiosurgery: is a differential diagnosis possible? J Neurosurg 2003;98:1056–64.

[4] Valk PE, Budinger TF, Levin VA, Silver P, Gutin PH, Doyle WK. PET of malignant cerebral tumors after interstitial brachytherapy. Demonstration of metabolic activity and correlation with clinical outcome. J Neurosurg 1988;69:830–8.

[5] Barai S, Bandopadhayaya GP, Julka PK, Naik KK, Haloi AK, Kumar R, et al. Role of Tc-glucoheptonic acid brain single photon emission computed tomography in differentiation of recurrent brain tumour and post-radiation gliosis. Australas Radiol 2004;48:296–301.

[6] Kline JL, Noto RB, Glantz M. Single-photon emission CT in the evaluation of recurrent brain tumor in patients treated with gamma knife radiosurgery or conventional radiation therapy. Am J Neuroradiol 1996;17:1681–6.

[7] Serizawa T, Saeki N, Higuchi Y, Ono J, Matsuda S, Yanagisawa M, et al. Diagnostic value of thallium-201 chloride single-photon emission computerized tomography in differentiating tumor recurrence from radiation injury after gamma knife surgery for metastatic brain tumors. J Neurosurg 2005;102:266–71.

[8] Rock JP, Hearshen D, Scarpace L, Croteau D, Gutierrez J, Fisher JL, et al. Correlations between magnetic resonance spectroscopy and image-guided histopathology, with special attention to radiation necrosis. Neurosurgery 2002;51:912–20.

[9] Dethy S, Goldman S, Blecic S, Luxen A, Levivier M, Hildebrand J. Carbon-11-methionine and fluorine-18-FDG PET study in brain hematoma. J Nucl Med 1994;37:1162–6.

[10] Ogawa T, Hatazawa J, Inugami A, Murakami M, Fujita H, Shimosegawa E, et al. Carbon-11-methionine PET evaluation of intracerebral hematoma: distinguishing neoplastic from non-neoplastic hematoma. J Nucl Med 1995;36:2175–9.

[11] Iwai Y, Yamanaka K, Oda J, Tsuyuguchi N, Ochi H. Tracer accumulation in radiation necrosis of the brain after thallium-201 SPECT and [11C]methionine PET-case report. Neurol Med Chir 2001;41:415–8.

[12] Sinha S, Bastin ME, Whittle IR, Wardlaw JM. Diffusion tensor MR imaging of high-grade cerebral gliomas. Am J Neuroradiol 2002;23:520–7.

[13] Beppu T, Inoue T, Shibata Y, Kurose A, Arai H, Ogasawara K, et al. Measurement of fractional anisotropy using diffusion tensor MRI in supratentorial astrocytic tumors. J Neurooncol 2003;63:109–16.

[14] Misaki T, Beppu T, Inoue T, Ogasawara K, Ogawa A, Kabasawa H. Use of fractional anisotropy value by diffusion tensor MRI for preoperative diagnosis of astrocytic tumors: case report. J Neurooncol 2004;70:343–8.

[15] Beppu T, Inoue T, Shibata Y, Yamada N, Kurose A, Ogasawara K, et al. Fractional anisotropy value by diffusion tensor magnetic reso-

nance imaging as a predictor of cell density and proliferation activity of glioblastomas. Surg Neurol 2005;63:56–61.
[16] Inoue T, Ogasawara K, Beppu T, Ogawa A, Kabasawa H. Diffusion tensor imaging for preoperative evaluation of tumor grade in gliomas. Clin Neurol Neurosurg 2005;107:174–80.
[17] Pierpaoli C, Basser PJ. Toward a quantitative assessment of diffusion anisotropy. Magn Reson Med 1996;36:893–906.
[18] Papadakis NG, Xing D, Houston GC, Smith JM, Smith MI, James MF, et al. A study of rotationally invariant and symmetric indices of diffusion anisotropy. Magn Reson Med 1999;17:881–92.
[19] Sorensen AG, Wu O, Copen WA, Davis TLGonzalez RG, Koroshetx WJ, Reese TG, et al. Human acute cerebral ischemia: detection of changes in water diffusion anisotropy by using MR imaging. Radiology 1999;212:785–92.
[20] Werring DJ, Clark CA, Parker GJ, Miller DH, Thompson AJ, Barker GJ. A direct demonstration of both structure and function in the visual system: combining diffusion tensor imaging with functional magnetic resonance imaging. Neuroimage 1999;9:352–61.
[21] Pierpaoli C, Jezzard P, Basser PJ, Barnett A, Di Chiro G. Diffusion tensor MR imaging of the human brain. Radiology 1996;201: 637–48.
[22] Witwer BP, Moftakhar R, Hasan KM, Deshmukh P, Haughton V, Field A, et al. Diffusion-tensor imaging of white matter tracts in patients with cerebral neoplasm. J Neurosurg 2002;97: 568–75.
[23] Yasargil MG, Microneurosurgery IV A (in 4 vol.). Georg Thieme, Stuttgart/New York Verlag (for distribution in Japan: Nankodo Company Ltd., Tokyo; 1993. p. 127).

J Neurosurg (Suppl) 105:86–90, 2006

Gamma Knife surgery for metastatic brain tumors without prophylactic whole-brain radiotherapy: results in 1000 consecutive cases

TORU SERIZAWA, M.D., PH.D., YOSHINORI HIGUCHI, M.D., PH.D., JUNICHI ONO, M.D., PH.D., SHINJI MATSUDA, M.D., PH.D., OSAMU NAGANO, M.D., YASUO IWADATE, M.D., PH.D., AND NAOKATSU SAEKI, M.D., PH.D.

Gamma Knife House, Departments of Neurosurgery and Neurology, Chiba Cardiovascular Center, Ichihara; and Department of Neurological Surgery, Graduate School of Medicine, Chiba University, Chiba, Japan

Object. The authors analyzed the effectiveness of Gamma Knife surgery (GKS) for metastatic brain tumors without adjuvant prophylactic whole-brain radiotherapy (WBRT). Salvage GKS was performed as the sole treatment for new distant lesions.

Methods. Among 1127 patients in whom new brain metastases had been diagnosed, 97 who met one or more of the following three criteria were excluded from the study: any surgically inaccessible huge (≥ 35 mm) lesion; tumor number and size requiring an internal skull dose exceeding 10 J; or symptomatic carcinomatous meningitis. Thus, 1030 consecutive patients formed the basis for this study. Huge tumors were totally removed, whereas smaller lesions were treated with GKS. No adjuvant WBRT was given prior to GKS, and new distant lesions were appropriately retreated with GKS. Overall, neurological and new lesion–free survival curves were calculated and the prognostic values of covariates were obtained. In total, 1853 separate GKS sessions were required to treat 10,163 lesions.The patients' median overall survival period was 8.6 months. Neurological survival and new lesion–free rates at 1 year were 89.1 and 49.3%, respectively. In a multivariate analysis, the significant factors for poor prognosis were the development of more than four new brain metastases and active extracranial disease.

Conclusions. In meeting the goal of preventing neurological death and maintaining activities of daily living for patients with brain metastases, GKS alone provides excellent palliation without prophylactic WBRT. New distant lesions were quite well controlled with GKS salvage treatment alone.

KEY WORDS • **metastatic brain tumor** • **stereotactic radiosurgery** • **Gamma Knife surgery** • **whole-brain radiotherapy** • **neurological survival**

We previously reported on the effectiveness and limitations of GKS without the addition of prophylactic WBRT, especially in patients with lung cancer.[5–7] The present study provides a rather large data set based on treatment with GKS alone for brain metastases from various primary cancers. All cancer types were treated according to the same protocol, with the focus being on new distant lesions and salvage GKS.

Clinical Material and Methods

Among 1127 patients in whom new brain metastases had been diagnosed, 97 who met one or more of the following three criteria were excluded from the study: any patient with a surgically inaccessible huge (≥ 35 mm) lesion; any patient with a tumor number and size requiring a TSID exceeding 10 J; or any patient with symptomatic carcinomatous meningitis. Thus, 1030 consecutive patients formed the basis for this study. Huge tumors were totally removed, whereas smaller lesions were treated with GKS. No adjuvant WBRT was given prior to GKS. New distant lesions, detected on MR imaging performed every 2 to 3 months, were appropriately retreated with GKS, if the patient's condition allowed. The TSID calculated with the Leksell Gamma Plan (Elekta Instruments, Norcross, GA) for each radiosurgical procedure was less than 10 J, thus preventing acute brain swelling, as previously reported.[5–7] The patients' primary physicians determined chemotherapy protocols. Neurological evaluations and Gd-enhanced MR imaging were performed every 2 to 3 months until the patient's KPS score was below 70. Thereafter, enhanced MR images were obtained at the primary hospital for as long as possible and sent to us for evaluation. The dates and causes

Abbreviations used in this paper: ADL = activities of daily living; CSF = cerebrospinal fluid; HR = hazard ratio; KPS = Karnofsky Performance Scale; MR = magnetic resonance; NLFS = new lesion–free survival; NS = neurological survival; OS = overall survival; QS = quality of survival; TSID = total skull internal dose; WBRT = whole-brain radiotherapy.

of death and progression of impaired ADL were documented by the patients' primary physicians. Control of the GKS-treated lesion was defined as the absence of any significant increase in tumor diameter (< 20%). Thallium-201 chloride single-photon emission computed tomography, as previously reported,[8] was used to differentiate tumor recurrence from radiation injury. The definitions of tiny, small, medium, and large lesions were as follows: less than or equal to 1 cm, greater than 1 cm but less than or equal to 2 cm, greater than 2 cm but less than or equal to 3 cm, and greater than 3 cm, respectively. Neurological death was defined as death due to any form of intracranial disease, including tumor recurrence, carcinomatous meningitis, cerebral dissemination, and other unrelated intracranial diseases, as described by Patchell, et al.[4] Impaired ADL function was defined as neurological status based on a KPS score of less than 70 (functional preservation), as reported by Aoyama and coworkers.[1]

Statistical Analysis

The intervals from the date of diagnosis of brain metastases at our center until the date of death (OS), neurological death (NS), impaired ADL (QS), and the appearance of new distant lesions (NLFS) were calculated using the Kaplan–Meier method. Tumor progression–free survival in all patients treated with GKS during the observation period was also analyzed. Prognostic values of the individual covariates for OS, NS, QS, and NLFS were obtained with the Cox proportional-hazards model. The following 12 dichotomized covariates were entered: age (< 65 years compared with ≥ 65 years); sex (male compared with female); extracranial lesion status (controlled compared with active); pretreatment KPS score (< 70 compared with ≥ 70); primary cancer organ (lung compared with nonlung); number of brain lesions (≤ four compared with > four); maximum lesion diameter (< 25 mm compared with ≥ 25 mm); initial total tumor volume (≤ 10 cm^3 compared with >10 cm^3); MR imaging findings of CSF dissemination (yes compared with no); chemotherapy (yes compared with no); craniotomy (yes compared with no); and time elapsed between diagnosis of primary cancer and brain metastases (synchronous compared with metachronous). A probability value of less than 0.001 was taken to represent a statistically significant difference.

Results

The distributions of patient characteristics and lesion types and locations are summarized in Table 1. The primary organs were the lung in 719 patients (69.8%), gastrointestinal in 124 (12.3%), breast in 68 (6.6%), urinary tract in 52 (5%), and others/undetermined in 67 (6.5%). The median number of lesions treated with the initial GKS was three (range one–25 lesions). During the follow-up period, the number of GKS procedures for new distant lesions averaged 1.8 ± 1.5, varying between one and 18, and the mean number of lesions treated with GKS per patient was 9.9 ± 16.6 (range one–109). In total, 1853 separate GKS procedures were required to treat 10,163 lesions. The mean calculated tumor volume was 0.87 ± 2.64 cm^3 (median 0.08 cm^3; range 0.1–24 cm^3).

TABLE 1

*Dichotomized patient characteristics**

Characteristic	No. of Patients
age (yrs)	
<65	547
≥65	483
sex	
male	654
female	376
extracranial disease	
controlled	125
active	905
pretreatment KPS score	
<70	162
≥70	868
primary organ	
lung	719
nonlung	311
no. of lesions	
≤4	620 (single 276)
>4	410
max lesion size (mm)	
<25	675
≥25	355
total tumor vol (cm^3)	
≤10	757
>10	273
CSF dissemination	
yes	86
no	944
chemotherapy	
yes	409
no	621
craniotomy	
yes	145
no	885
metastasis	
synchronous	385
metachronous	645

The minimum dose to the tumor margin was 15 to 30 Gy (mean ± standard deviation 20.4 ± 2.0 Gy; median 20 Gy) with a 72.4% isodose contour (range 30–98%). The mean prescribed doses were 20.6 Gy in 8573 tiny, 20.3 Gy in 977 small, 19.2 Gy in 441 medium, and 15.7 Gy in 172 large lesions. Figure 1 shows the cumulative lesion progression-free survival curves stratified by lesion size. The tumor control rates at 1 year were 99.5% in tiny, 92.6% in small, 87.3% in medium, and 65.5% in large lesions. The differences were statistically significant ($p < 0.0001$). Among 184 lesions showing progression, we diagnosed tumor recurrence in 83 and radiation injury in 101. The median OS period was 8.6 months. In multivariate analysis, significant prognostic factors for OS were active extracranial disease ($p < 0.0001$, HR 4.184), low pretreatment KPS score ($p < 0.0001$; HR 2.050), and male sex ($p < 0.0001$; HR 1.561). The OS curves were compared by using the Radiation Therapy Oncology Group recursive partitioning analysis classes (Fig. 2). The neurological death–free rates were 89% at 1 year and 73.6% at 2 years. Among the 729 deaths, 125 (17.1%) were attributed to neurological death (NS). Causes of neurological death were carcinomatous meningitis in 54, recurrence of the treated lesion in 29, cerebral dissemination in 22, progression of an untreated lesion in 16, and other in four. The only significant poor prognostic factor for NS was carcinomatous

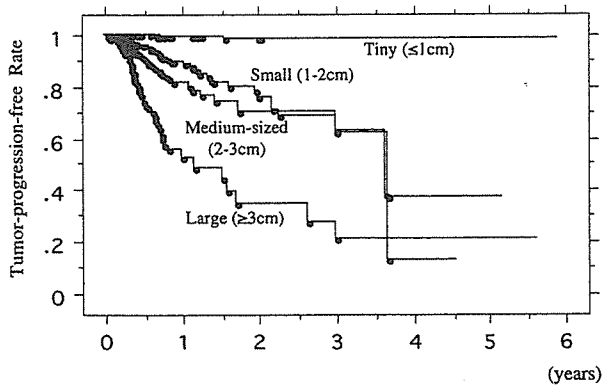

FIG. 1. Graph showing cumulative tumor progression–free survival curves, based on tumor size. The maximum lesion diameters are provided. The mean prescribed doses were 20.6 Gy in 8573 tiny, 20.3 Gy in 977 small, 19.2 Gy in 441 medium, and 15.7 Gy in 172 large lesions. The tumor control rates at 1 year were 99.5% in tiny, 92.6% in small, 87.3% in medium, and 65.5% in large lesions. Differences were statistically significant ($p < 0.0001$).

meningitis ($p < 0.0001$, HR 4.841). The NS curves were compared between patients with and without MR imaging findings of carcinomatous meningitis (Fig. 3). The QS rates were 82.1% at 1 year and 62.9% at 2 years. The MR imaging findings of CSF dissemination ($p < 0.0001$; HR 3.305) and active extracranial disease ($p < 0.0001$; HR 2.237) were confirmed to be significant factors influencing QS. No patient suffered radiation-induced dementia in this study. The NLFS rate at 1 year was 49.3%. According to multivariate analysis, the significant poor prognostic factors for NLFS were more than four brain metastases and active extracranial disease (Table 2). The NLFS curves based on tumor number are shown in Fig. 4. Among the 729 patients who died, the number of salvage GKS treatments for new distant lesions was zero in 470, one in 134, two in 62, three in 26, and more than four in 37. Salvage WBRT was subsequently performed in 30 patients with cerebral dissemination or CSF dissemination, which had been uncontrolled after aggressive GKS salvage treatment.

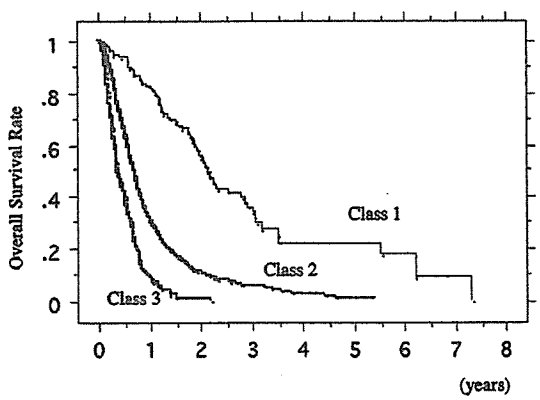

FIG. 2. Graph showing the OS curves stratified by Radiation Therapy Oncology Group recursive partitioning analysis classes. The median OS period was 2.2 years in Class 1, 0.71 years in Class 2, and 0.39 years in Class 3. Differences among the three classes were statistically significant ($p < 0.0001$).

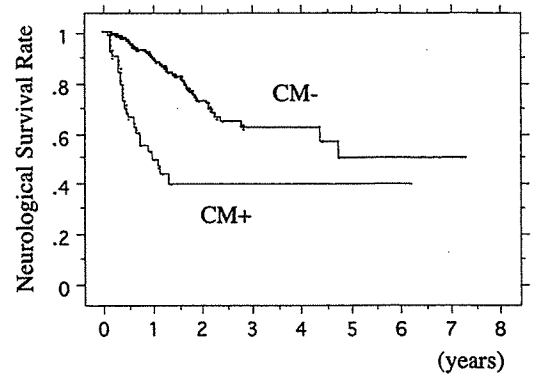

FIG. 3. Graph showing NS curves for patients with and without MR imaging evidence of carcinomatous meningitis. The neurological death–free rates at 1 year were 90.2% in patients with carcinomatous meningitis and 52.4% in those without. The difference was statistically significant ($p < 0.0001$). CM = carcinomatous meningitis.

Discussion

A few retrospective, randomized, controlled studies in which radiosurgery and radiosurgery plus initial adjuvant WBRT were compared have been reported.[1–3,9,10] In the Japanese Radiation Oncology Study Group series reported on by Aoyama, et al.,[1] no significant differences were found in OS, NS, or QS between radiosurgery alone and radiosurgery after adjuvant WBRT, although new lesions were observed more frequently with radiosurgery alone. These results support our treatment protocol of using GKS aggressively, at least in patients with only a few metastases. Our study comprised a very large series of patients who underwent GKS and did not receive any initial adjuvant WBRT. All patients were treated using the same treatment protocol. We have carefully analyzed the results and focused particular attention on new distant lesions.

New Distant Lesions and Salvage Treatment

Since the advent of computed tomography scanning, it has come to be widely believed that even patients with only a single metastatic lesion harbor microscopic

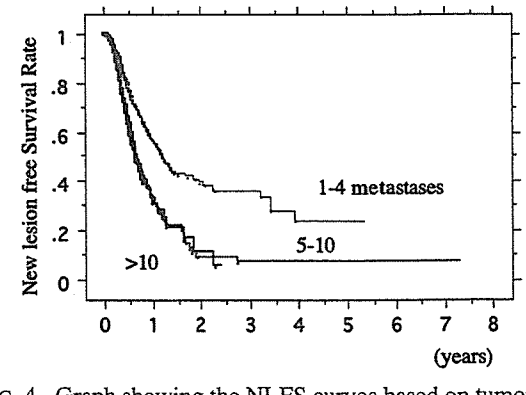

FIG. 4. Graph showing the NLFS curves based on tumor number. The new lesion–free rates at 1 year were 57.2% in patients with one to four brain metastases, 34.2% in those with five to 10, and 32.9% in those with more than 10. The difference between one to four and more than four brain metastases was statistically significant ($p < 0.0001$).

TABLE 2
Prognostic variables for NLFS

Variable	High Risk Group	p Value*	HR*	p Value†	HR†
age	<65	0.0441	1.229		
sex	male	0.4949	1.073		
extracranial disease	active	<0.0001	1.835	0.0005	1.656
initial KPS score	≥70	0.3603	1.161		
primary site	lung	0.9933	1.001		
no. of lesions	>4	<0.0001	1.844	<0.0001	1.734
max lesion size	<25 mm	0.9394	1.016		
total tumor vol	>10 cm^3	0.0826	1.316		
CSF dissemination	no	0.3327	1.232		
chemotherapy	yes	0.5884	1.057		
craniotomy	no	0.7755	1.038		
metastasis	synchronous	0.6298	1.052		

*Values are based on univariate analysis.
†Values are based on multivariate analysis (Cox proportional-hazards model).

metastases.[2,3] Modern high-resolution MR imaging can detect tumors only a few millimeters in diameter, and even these tiny metastatic lesions can be safely and accurately treated with GKS. The patient survival period may be too short for invisible metastases or true new lesions to be identified on follow-up MR imaging or to cause neurological symptoms. Chemotherapy may, of course, play an additional role in controlling microscopic lesions, especially in cancers sensitive to chemotherapy, such as small cell lung cancer and breast cancer. Our experience suggests that local control is the most important clinical goal for patients with brain metastases and that it is not necessary to treat invisible metastases. Indeed, approximately two-thirds of patients in this series did not require salvage treatment. If new lesions are detected, appropriate salvage treatment, taking patient condition into consideration, may be warranted. Whole-brain radiotherapy should be used only with great caution because of its invasive nature. The current study demonstrates that a local GKS treatment protocol without upfront WBRT can provide highly satisfactory results in selected patients.

Cost of GKS Alone Protocol

The cost of any local treatment protocol, without prophylactic WBRT, must always be considered. In Japan, GKS is relatively inexpensive, approximately 4000 US dollars; WBRT is less expensive and costs closer to 2500 US dollars. In this series, the mean number of GKS salvage treatments for new distant lesions was 0.8 per patient. The incidence of new distant lesions that can be controlled using GKS is expected to be 50%, provided all invisible microscopic lesions are controlled by initial WBRT. Thus, the total treatment costs come to approximately 7200 US dollars for GKS without prophylactic WBRT ($4000 + 4000 \times 0.8$) and 8100 US dollars for GKS with prophylactic WBRT ($4000 + 2500 + 4000 \times 0.4$). This local treatment is thus estimated to be less expensive than GKS with initial WBRT, although some patients may require frequent salvage GKS. The Japanese public insurance system covers all initial and salvage GKS procedures as well as follow-up MR imaging. Economic factors impacting radiosurgery and radiotherapy apparently differ markedly among countries. If the portions of fees for radiosurgery and radiotherapy covered by health insurance are similar to those in Japan, the cost of our local treatment protocol without prophylactic WBRT would appear to be quite reasonable.

Indications for and Limitations of our Local Treatment Protocol

Factors that limit the performance of single-session GKS include not only the number but also the size of lesions. Earlier reviews focused solely on number of lesions. To resolve this problem, we have proposed the TSID concept, which provides information on the limitations of safe GKS in a single session.[5–7] A TSID of 10 J is equivalent to 3 Gy of whole-skull radiation or a total tumor volume of 15 cm^3. This is also the WBRT single-fraction dose used for metastatic brain tumors (30 Gy in 10 fractions). If the lesions are scattered diffusely and similar of size, 25 tiny, 10 small, or four medium lesions would be the treatment limits of a single GKS session, assuming the peripheral doses are all 20 Gy. Adverse early radiation effects such as acute brain swelling were not observed in the present series with the TSID below 10 J. Yamamoto and colleagues[11] and Yang and coworkers,[12] although using higher radiation doses than allowed by our criteria, reported the safety of GKS for numerous brain metastases. The present criteria exclude patients with symptomatic carcinomatous meningitis, but thin-slice MR imaging for dose planning revealed asymptomatic CSF dissemination to be a highly significant poor prognostic factor for NS and QS. Thus, the exclusion criteria for this treatment are any surgically inaccessible huge (≥ 35 mm) tumor; tumor number and size exceeding a TSID of 10 J; and MR imaging findings of CSF dissemination. More than four brain metastases and active extracranial lesions were recognized as poor prognostic factors for new distant lesions on multivariate analysis. However, having more than four metastases did not affect OS, NS, or QS on multivariate analysis. For patients with more than four metastases, a randomized controlled study in which GKS alone is compared with GKS plus initial adjuvant WBRT should be performed.

Conclusions

In terms of NS and QS, GKS without initial adjuvant WBRT for brain metastases from various primary cancers provides excellent palliation considering the patients' short life expectancies. New distant lesions were fairly

well controlled with GKS salvage treatment alone, even in patients with more than four brain metastases; however, careful observation with enhanced MR imaging at intervals of no more than 3 months is necessary.

References

1. Aoyama H, Shirato H, Tago M, Nakagawara K, Toyoda T, Hatano K, et al: Stereotactic radiosurgery plus whole brain radiation therapy vs stereotactcic radiosurgery alone for treatment of brain metastases: a randomized controlled trial. **JAMA 295:**2483–2491, 2006
2. Arriagada R, Le Chevalier T, Borie F, Riviere A, Chomy P, Monnet I, et al: Prophylactic cranial irradiation for patients with small-cell lung cancer in complete remission. **J Nat Cancer Inst 87:**183–190, 1995
3. Kondziolka D, Patel A, Lunsford LD, Kassam A, Flickinger JC: Stereotactic radiosurgery plus whole brain radiotherapy versus radiotherapy alone for patients with multiple brain metastases. **Int J Radiat Oncol Biol Phys 45:**427–737, 1999
4. Patchell RA, Tibbs PA, Walsh JW, Dempsey RJ, Maruyama Y, Kryscio RJ, et al: A randomized trial of surgery in the treatment of single metastases to the brain. **N Engl J Med 322:**494–500, 1990
5. Serizawa T, Iuchi T, Ono J, Saeki N, Osato K, Odaki M, et al: Gamma Knife treatment for multiple metastatic brain tumors compared with whole-brain radiation therapy. **J Neurosurg (Suppl 3) 93:**32–36, 2000
6. Serizawa T, Ono J, Iuchi T, Matsuda S, Sato M, Odaki M, et al: Gamma Knife radiosurgery for metastatic brain tumors from lung cancer. Comparison between small cell cancer and non-small cell cancer. **J Neurosurg (Suppl 5) 97:**484–488, 2002
7. Serizawa T, Saeki N, Higuchi Y, Ono J, Iuchi T, Nagano O, et al: Gamma Knife surgery for brain metastases: indications for and limitations of a local treatment protocol. **Acta Neurochir (Wien) 147:**721–726, 2005
8. Serizawa T, Saeki N, Higuchi Y, Ono J, Matsuda S, Sato M, et al: Diagnostic value of thallium-201 chloride single-photon emission computed tomography in differentiating tumor recurrence from radiation injury after Gamma Knife surgery for metastatic brain tumors. **J Neurosurg (Suppl 2) 102:** 266–271, 2005
9. Sneed PK, Lamborn KR, Forstner JM, McDermott MW, Chang S, Park E, et al: Radiosurgery for brain metastases: is whole brain radiotherapy necessary? **Int J Radiat Oncol Biol Phys 43:**549–558, 1999
10. Sneed PK, Suh JH, Goetsch SJ, Sanghavi SN, Chappell R, Buatti JM, et al: A multi-institutional review of radiosurgery alone vs. radiosurgery with whole brain radiotherapy as the initial management of brain metastases. **Int J Radiat Oncol Biol Phys 53:**519–526, 2002
11. Yamamoto M, Ide M, Nishio S, Urakawa Y: Gamma Knife radiosurgery for numerous brain metastases: Is this a safe treatment? **Int J Radiat Oncol Biol Phys 53:**1279–1283, 2002
12. Yang CC, Ting J, Wu X, Markoe A: Dose volume histogram analysis of Gamma Knife radiosurgery treating twenty-five metastatic intracranial tumors. **Stereotac Funct Neurosurg 70:**41–49, 1998

Address reprint requests to: Toru Serizawa, M.D., Ph.D., Department of Neurosurgery, Chiba Cardiovascular Center, 575 Tsurumai, Ichihara, Chiba, 2900512 Japan. email: gamma-knife.serizawa@nifty.com.

Glioblastomaに対する薬剤感受性に基づいた個別化治療

Individualized treatment for glioblastoma based on drug sensitivity

千葉大学 脳神経外科学[1)]、千葉大学 病態病理学[2)]、
千葉県がんセンター研究局 化学療法部[3)]

岩立 康男[1)]、松谷 智朗[1)]、永井 雄一郎[2)]、藤本 修一[3)]、佐伯 直勝[1)]

【Summary】

Efficacy of chemotherapy against glioblastoma is still limited. To investigate whether individualization of chemotherapy according to drug sensitivity improves the outcome of patients with glioblastoma, 74 consecutive patients with glioblastoma who received individualized chemotherapy were retrospectively compared with 68 patients treated with the conventional nitrosourea plus cisplatin chemotherapy. For individualization, the drug-induced apoptosis from 31 anticancer drugs was quantified by flow-cytometry in the primary culture of surgically-resected tumor cells. The patients who received the individualized chemotherapy had significantly longer overall survival than those treated with the conventional chemotherapy ($p<0.0001$). The median survival of patients with glioblastoma was 19.4 months in the individualized chemotherapy group and 13.1 months in the conventional chemotherapy group. This study suggests an important new direction in glioblastoma chemotherapy; individualization of chemotherapy based on drug sensitivity is one of the important approaches to obtain prolonged survival in glioblastoma.

【はじめに】

Glioblastomaに対する化学療法は、blood brain-barrier (BBB)の透過性に優れたニトロソウレアを中心とした薬剤が選択されてきたが、その治療効果はけっして十分ではなかった[1-5]。近年、新規薬剤であるTemozolomideが、無作為化比較試験においてglioblastomaに対し有意な生存期間の延長効果を示したことが報告されたが、その延長効果も2ヶ月程度にとどまっている[6]。今後、本薬剤が悪性グリオーマの化学療法において重要な選択肢となっていくと思われるが、更なる治療成績の向上には、新しい治療戦略の開発が必須である。

近年の分子生物学の発展により、グリオーマを含めた癌一般の発生・進展に関わる遺伝子変異や遺伝子発現が、同一疾患でも均一ではないことが明らかにされた。将来的には、病理組織学的所見のみに基づいていた疾患単位に、分子レベルでの客観的な分類基準が与えられることが期待される。また同時に、種々の薬剤に対する感受性や耐性と関連する遺伝子もいくつか同定され[8-16]、個々の症例の遺伝子異常のパターンに応じて治療法を選択する"テーラーメイド治療"の実現が期待されている。しかしながら、個々の分子と薬剤への反応性という生物学的特性がどのように対応するか、という問題は複雑であり、現在得られている情報は断片的である。

我々は、glioblastomaに対して、腫瘍細胞の初代培養によるin vitro抗癌剤感受性試験を行い、その結果に基づいて薬剤を選択して使用する"個別化化学療法"を行ってきた[17]。今回、我々の抗癌剤感受性試験に基づく化学療法をテーラーメイド治療の一つのモデルとし、その治療効果をニトロソウレアを中心とした現時点での標準治療と比較検討した。

【対象と方法】

患者：病理診断が確定し、1年以上の経過観察が可能であったglioblastoma連続74例を対象とした。これら抗癌剤感受性試験の結果に基づいて治療された症例を個別化群とし、本法導入以前にACNUとcisplatinを中心に治療された68例をコントロール群として、retrospectiveな比較検討を行った。

抗癌剤感受性試験：腫瘍組織を摘出後直ちに細切し、single cell suspensionに近い状態とし、31種類の薬剤を臨床常用量における最高血中濃度[18]およびその10分の1濃度で8時間接触させた後、薬剤を含まない培地(RPMI 1640)で追加培養を行った。裸核処理後Propidium Iodide(PI)にてDNA染色を行い、フローサイトメーター(FACScan)にて核DNA量を測定した。効果判定はDNAヒストグラムにおけるsub-G_1 peakの上昇(アポトーシス細胞の増加)およびこれに伴うG_0/G_1ピークの低下(正常細胞の減少)を指標とした[19-23]。同時に、薬剤処理後の細胞をギムザ染色し、細胞形態

(核断裂像、核濃縮像)を観察することによりアポトーシス細胞の比率を測定した。

治療法：有効薬剤のうち作用機序の異なるものを2~3剤選択し、臨床常用量にて使用した。有効薬剤の存在しない症例では、ACNUとビンクリスチン、プロカルバジンを併用するPAV療法を行った。第一回目の化学療法は60Gyの放射線療法とともに行い、全身状態の許す限り維持化学療法を行った。また、コントロール群の化学療法は、ACNUとcisplatinを併用した固定レジメンを用いた。

統計学的検討：Kaplan-Meier法により生存率を算出し、Logrank検定にて有意差検定を行った。

【結 果】

予後に関連すると思われる患者背景因子は両群間で有意差を認めなかった(Table 1)。

有効薬剤は症例毎に異なっていた。glioblastomaにおける31薬剤の陽性率をFig.1に示す。以前に行ったanaplastic astrocytoma(AA)25例のデータと比較した結果、抗癌剤感受性は、全般にAAの方がglioblastomaよりも高かった。ACNUの有効率はAAで20%、glioblastomaで5%であり、両組織型間で統計学的有意差を認めた。MCNU、cisplatinの有効率は両群間で差がなくMCNUで6-7%程度、シスプラチン15-16%であった。Glioblastomaに対して最も有効率の高かったのはpacritaxelで23%、続いてaclarubicinの22%であった。

肉眼的全摘出の施行しえた症例の中に、ある程度の長期生存例がみられた(Fig.2)。一方、術前の画像で脳梁を介した反対側への浸潤が見られる症例は、感受性試験で全薬剤無効となる場合が多く、放射線治療・ACNUを中心とした化学療法にもかかわらず急速な再発を認めた(Fig.3)。全体としての生存期間中央値は、個別化群19.4ヶ月、コントロール群13.1ヶ月であり、個別化群で有意な生存期間の延長が認められた(P<0.0001)(Fig.4)。しかしながら、長期生存期間を見てみると、個別化群の5年生存率は10%以下であり、コントロール群との間に差を認めなかった。

Table 1

Patients characteristics

	Conventional	Individualized
N	68	74
Age		
Mean	53.3	51.5
Range	18-78	15-77
Sex		
Male	47 (69%)	49 (66%)
Female	21 (31%)	25 (34%)
KPS score		
Mean	75	76
Range	50-100	50-100
Tumor location		
Left	37 (54%)	37 (50%)
Right	27 (40%)	28 (38%)
Midline	4 (6%)	9 (12%)
Extent of surgery		
Total/Subtotal	35 (52%)	46 (62%)
Partial/Biopsy	33 (48%)	28 (38%)

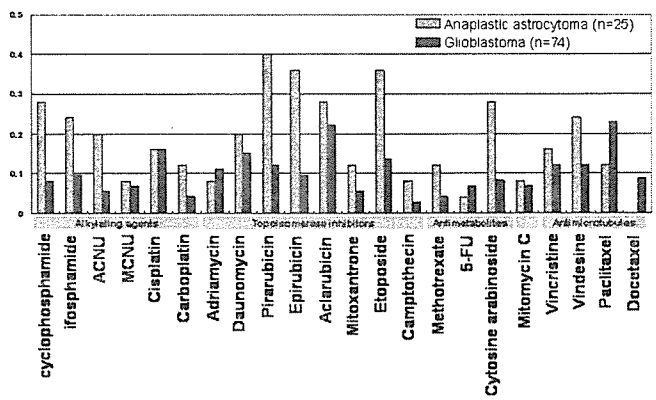

Fig.1

Effective rates of each anticancer drugs

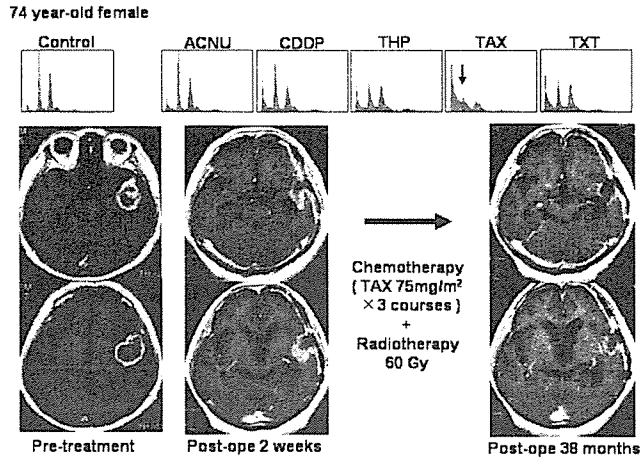

Fig.2

A representative case with effective drugs in vitro. Paclitaxel selected by the drug-sensitivity test was administered.

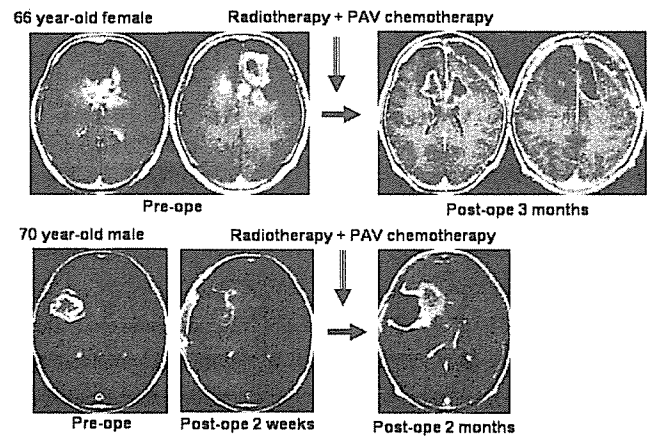

Fig.3

A representative case without effective drugs in vitro. PAV chemotherapy using ACNU, procarbazine, and vincristine was administered.

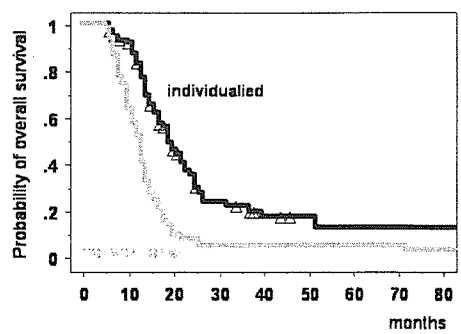

Fig.4

Kaplan-Meier estimated probability of overall survival rate of the patients with glioblastoma multiforme treated either with individualized chemotherapy or conventional chemotherapy using ACNU and cisplatin.

【考 察】

今回の結果から、Glioblastomaにおける個別化群の生存期間は、ニトロソウレアとプラチナ製剤を用いたコントロール群に比して有意に延長していた。また、生存期間中央値19.4ヶ月という数値は、当初の予想よりも短かったものの、ニトロソウレア剤を中心に治療されたこれまでの報告と比べ良好であった。本研究は無作為化比較試験でないためその解釈には慎重を要するが、glioblastomaに対する化学療法は、ニトロソウレア中心のレジメンよりも症例毎に個別化を図った方が有利である可能性が示唆された。日本におけるニトロソウレア剤であるACNUは、anaplastic astrocytomaやoligodendrogliomaに対してある程度の有効性を示すが、glioblastomaに対しては有効性が十分でないことはすでに多くの報告がある[1-5]。全ての悪性グリオーマに対し、ACNUを無条件に第一選択剤とする治療法は、患者にとってメリットが少ないと考えられる。近年、海外においてglioblastomaに対する生存期間延長効果の証明されたtemozolomideが日本でも使用可能となった。今後、本薬剤は、悪性グリオーマの化学療法における標準的治療薬として有力な選択肢となっていくであろう。

ニトロソウレア剤に耐性を与えるO^6-methylguanine-DNA methytransferase（MGMT）の腫瘍細胞における発現量を測定し、治療法の選択に応用しようという試みもなされている[24]。この方法は、作用機序に関する理論が確立しているため、優れた方向性であるといえる。感受性因子と異なり、耐性因子は一つでも大量に存在すればその薬剤は無効となるはずである。一方、テーラーメイド化学療法においては、作用機序の異なる複数の治療選択肢を準備することが理想的である。すなわち、ある薬剤が効かない症例を探すだけでなく、効きそうな薬剤を積極的に探し出すシステムを構築する努力が必要であると考えられる。先のtemozolomideもMGMT高発現の腫瘍には効きづらいことが示されており[26]、こういった腫瘍をどのように治療していくかが今後大きな問題となってくるであろう。

薬剤の効果に影響する因子は、薬物代謝酵素、薬剤受容体、アポトーシス誘導、DNA修復酵素、シグナル伝達系など多岐にわたる分子が複雑なネットワークを形成していると考えられるため、一つないし少数の因子のみ解析しても、治療を個別化するための情報量としては不十分であると考えられる。今回、個別化の手法として我々が用いたのは、フローサイトメトリーを用いたアポトーシスの検出による薬剤感受性試験である[19-23]。本法は、基礎研究の場においてスタンダードなアポトーシス検出法として定着した技術であり、摘出された腫瘍から厳密な単細胞浮遊液を作製する必要がないことから、臨床応用するのに適した薬剤感受性試験である。しかしながら、in vitroの細胞培養による感受性測定は、in vivoの微小環境を反映しない点が最も根源的な問題点としてあげられる。今回の検討でも、長期生存の得られた症例は少数であり、化学療法を感受性試験に基づいて個別化することのメリットは最小限に止まったと考えられる。現有薬剤を用いた化学療法の限界もあるが、我々はより精度の高い感受性予測システムを構築しなければならない。摘出後直ちに凍結保存された腫瘍組織の遺伝子解析・遺伝子発現解析はin vivoの状態を正確に反映していると考えられる。我々は、既知の薬剤感受性因子・耐性因子をいくつか測定し、感受性試験の補助として用いることを検討中である。

【文 献】

1) Takakura K, Abe H, Nomura K, et al: Effects of ACNU and radiotherapy on malignant glioma. J Neurtosurg 64: 53-57, 1986
2) Levin VA, Silver P, Wilson CB, et al: Superiority of post-radiotherapy adjuvant chemotherapy with CCNU, procarbazine and vincristine (PCV) over BCNU for anaplastic gliomas: NCOG 6G61 final report. Int J Radiat Oncol Biol Phys 18: 321-324, 1990
3) Iwadate Y, Namba H, Sueyoshi K: Intra-arterial ACNU and cisplatin chemotherapy for the treatment of glioblastoma multiforme. Neurol Med Chir (Tokyo) 35: 598-603, 1995
4) Davis,F.G., Freels, S., Grutsch, J., et al. Survival rates in patients with primary malignant brain tumors stratified by patient age and tumor histological type: an analysis based on surveillance, epidemiology, and end results (SEER) data, 1973-1991. J.Neurosurg 88: 1-10, 1998.
5) Shapiro WR: Current therapy for brain tumors: back to the future. Arch Neurol 56: 429-432, 1999
6) Stupp R, Mason WP, van den Bent MJ, et al. Radiotherapy plus concomitant and adjuvant temozolomide for glioblastoma. N Engl J Med 352: 987-96, 2005.
7) Markert JM, Fuller CM, GIllespie GY, et al: Differential gene expression profiling in human brain tumors. Physiological Genomics 5: 21-33, 2001
8) Yung KWA, Shapiro JR, Shapiro WR: Heterogeneous chemosensitivities of subpopulations of human glioma cells in culture. Cancer Res 42: 992-998, 1982
9) Khan J, Wei JS, Meltzer PS, et al: Classification and diagnostic prediction of cancers using gene expression profiling and artificial neural networks. Nat Med 7: 673-679, 2001
10) James CD, Olson JJ: Molecular genetics and

molecular biology advances in brain tumors. Curr Opin Oncol 8: 188-195, 1995

11) Fojo AT, Ueda K, Pastan I, et al: Expression of a multidrug resistance gene in human tumors and tissues. Proc Natl Acad Sci USA 84: 265-269, 1987
12) Iwadate Y, Fujimoto S, Tagawa M, et al: Association of p53 gene mutation with decreased chemosensitivity in human malignant gliomas. Int J Cancer 69: 236-240, 1996
13) Iwadate Y, Mochizuki S, Yamaura A, et al: Alteration of CDKN2/p16 in human astrocytic tumors is related with increased susceptibility to antimetabolite anticancer agents. Int J Oncol 17: 501-505, 2000
14) Matsumoto Y, Takano M, Fojo T: Cellular adaptation to drug exposure: Evaluation of the drug-resistant phenotype. Cancer Res 57: 5086-5092, 1997
15) Esteller M, Garcia-Foncillas J, Herman JG, et al: Inactivationof the DNA-repair gene MGMT and the clinical response of gliomas to alkylating agents. N Engl J Med 343: 1350-1354, 2000
16) Scherf U, Ross DT, Weinstein JN, et al: A gene expression database for the molecular pharmacology of cancer. Nature Genet 2000; 24: 236-244.
17) Iwadate Y, Fujimoto S, Namba H, Yamaura A. Promising survival for patients with glioblastoma multiforme treated with individualised chemotherapy based on in vitro drug sensitivity testing. Br J Cancer 89: 1896-900, 2003.
18) Alberts DS, Chen HSG: Tabular summary of pharmacokinetic parameters relevant to in vitro drug assay. Alan R. Liss, New York, pp 351-359, 1980
19) Nicoletti I, Migliorati G, Pagliacci MC, et al. A rapid and simple method for measuring thymocyte apoptosis by propidium iodide staining and flow cytometry. J Immunol Meth 1991; 139: 271-279.
20) Darzynkiewicz Z, Bruno S, Traganos F, et al: Features of apoptotic cells measured by flow cytometry. Cytometry 13: 795-808, 1992
21) Sekiya S, Takamizawa H, Tokita H, et al. A newly developed in vitro chemosensitivity test (Nuclear damage assay): application to ovarian cancer. Gynecologic Oncol 40: 138-143, 1991.
22) Iwadate Y, Fujimoto S, Yamaura Y, et al: Prediction of drug cytotoxicity in 9L rat brain tumor by using flow cytometry with a deoxyribonucleic acid-binding dye. Neurosurgery 40: 782-788, 1997
23) Iwadate Y, Fujimoto S, Yamaura A. Differential chemosensitivity in human intracerebral gliomas measured by flow cytometric DNA analysis. Int J Mol Med 10: 187-92, 2002.
24) Tanaka S, Kamitani H, Hori T, et al: Preliminary Individual adjuvant therapy for gliomas based on the results of molecular biological analyses for drug-resistance genes. J Neuro-Oncol 46: 157-171, 2000
25) Hegi ME, Diserens AC, Gorlia T et al. MGMT gene silencing and benefit from temozolomide in glioblastoma. N Engl J Med 352:997-1003, 2005.

No Shinkei Geka, 34(9): 885-898, 2006

総説
Review

脳・血管周囲腔と新しい病態
—高磁場MR機による占拠性病変の観察から—*

佐伯 直勝[1)] 村井 尚之[1)] 岩立 康男[1)]
永井雄一郎[2)] 角南 兼朗[3)]

Key words perivascular space, brain tumor, cystic lesion, brain edema, MR imaging, lacunar infarct
No Shinkei Geka 34(9): 885-898, 2006

Ⅰ. 従来の血管周囲腔の画像とその意義

高磁場のMR機器が広く普及し，人・生体における微細な構造が観察可能になった．それにつれ，血管周囲腔に関与したMR像が数多く報告されるようになった．1990年代から血管周囲腔は，MR上の分布と画像所見に類似点があることから，大脳基底核や前交連付近のラクナ梗塞との鑑別疾患としてクローズアップされた．また，大脳白質(centrum semiovale)においては，境界不鮮明な地図状，斑状の白質病変であるleukoaraiosisとの鑑別が問題となっている[2,3,5,8,11,15]．

血管周囲腔は，MR上脳実質内での拡大した部分が観察され，画像上，脳表から多少離れた脳実質内の脳脊髄液信号域として観察される．血管周囲腔は以下の5つの条件を満たした際，それと診断される．

1) すべてのシーケンスで脳脊髄液の信号域を呈する．
2) 通常3 mm以下のサイズである．
3) 辺縁が鮮明である．
4) 血管走行と解剖学的に一致する．
5) mass effectはない[24,27]．

しかし，サイズに関しては，以下に述べるごとく大脳半球部のものでは2 cmに至るものや，多少の圧迫所見を有する場合があり，それを病的と取るか否かは，臨床所見を加味した総合的判断が必要な場合がある[25,37]．

1990年代の後半から，血管障害以外の中枢神経疾患で，血管周囲腔に関与した画像が報告されるようになった．アルツハイマー病を含む認知障害での血管周囲腔の果たす役割や，神経内科疾患では多発性硬化症のsand-like appearance，小児の偏頭痛で血管周囲腔が拡大することなどが報告されており，その病態との関連で注目されている[1,20,39]．脳腫瘍の画像や病態においても新しい知

* MR Studies of Perivascular Spaces with Main Emphasis on Space-occupying Lesions

1) 千葉大学大学院医学研究院脳神経外科学，Naokatsu Saeki, M.D., Ph.D., Hisayuki Murai, M.D., Ph.D., Yasuo Iwadate, M.D., Ph.D., Department of Neurosurgery, Chiba University Graduate School of Medicine
2) 千葉大学大学院医学研究院病態病理学，Yuichiro Nagai, M.D., Ph.D., Department of Pathology, Chiba University Graduate School of Medicine
3) JFE川鉄千葉病院脳神経外科，Kenro Sunami, M.D., Ph.D., Department of Neurosurgery, JFE Kawatetsu Chiba Hospital
〔連絡先〕佐伯直勝＝千葉大学大学院医学研究院脳神経外科（〒260-8670 千葉市中央区亥鼻1-8-1）
Address reprint requests to: Naokatsu Saeki, M.D., Ph.D., Department of Neurosurgery, Chiba University Graduate School of Medicine, 1-8-1 Inohana, Chuo-ku, Chiba-city, Chiba 260-8670, Japan

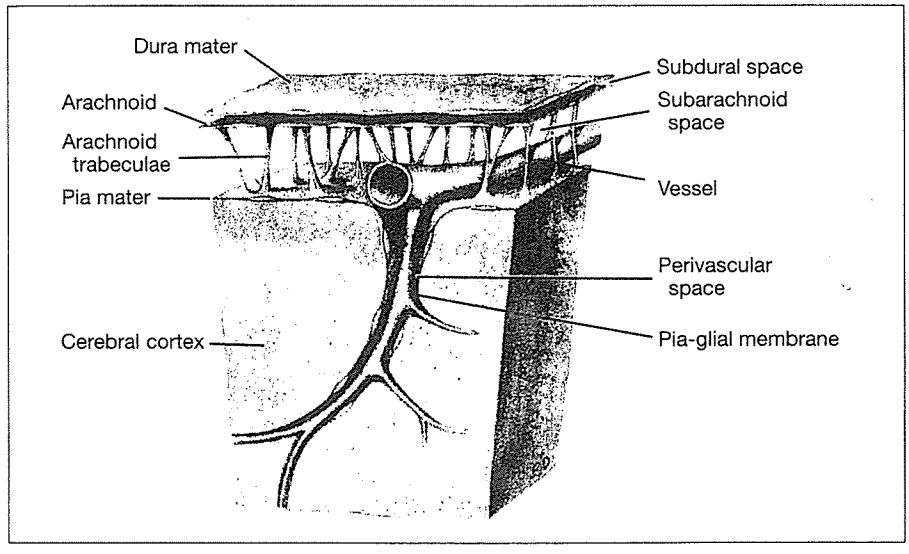

Fig. 1 Perivascular space in a textbook of neuroanatomy (modified from reference 29). In this drawing, subarachnoid space directly perforates the brain surface into the parenchyma. No detailed anatomy is elucidated in relation to subarachnoid space, pia mater, subpial space and perivascular space.

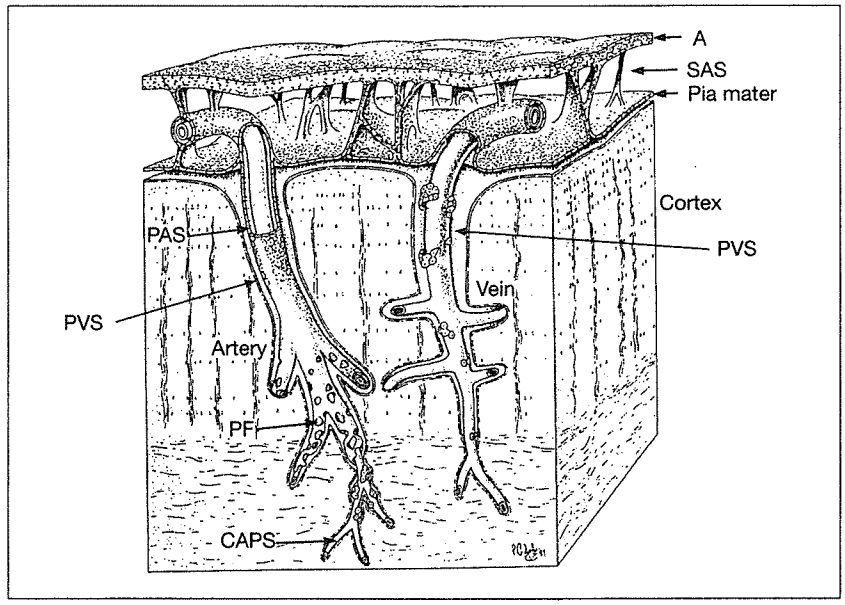

Fig. 2 Diagram demonstrating the relationships of the pia mater and intracerebral vessels (modified from reference 44). Subarachnoid space (**SAS**) separates the arachnoid (**A**) from the pia mater overlying the cerebral cortex. Perivascular space (**PVS**) of the artery(left picture). An artery on the left of the picture is coated by a sheath of cells derived from the **pia mater**:the sheath has been cut away to show that the periarterial spaces (**PAS**) of the intracerebral and extracerebral arteries are in continuity. The layer of the pial cells becomes perforated (**PF**) and incomplete as smooth muscle cells are lost from the smaller branches of the artery. The pial sheath finally disappears as the PVS are obliterated around the capillaries (**CAPS**). PVS of the vein (**right picture**). PVS around the vein are confluent with the subpial space. The picture shows that PVS are anatomically different around the artery and vein.

見が散見される．ここでは，腫瘍性病変と血管周囲腔の画像に関する最近の話題をレビューする．

II．血管周囲腔の解剖と動物実験による生理学的所見

血管周囲腔は，血管が脳表面を脳脊髄液腔を伴いながら穿通・通過する際に形成される．従来，解剖学的に血管周囲腔はくも膜下腔そのものが脳実質内に入り込むものとして理解されてきた[29]（Fig. 1）．しかし，1990年にZhangらは脳表のくも膜下腔の電子顕微鏡の観察から，血管周囲腔には動脈と静脈性のものがあり，軟膜，軟膜下腔との関係で解剖学的に違いがあることを指摘した[44]（Fig. 2）．動脈がくも膜下腔を通過し，軟膜を穿通し軟膜下腔から脳内に入るに従って軟膜細胞からなるlayerがperivascular sheathを形成する．動脈はそれに囲まれ被服される．このlayerは脳深部にいたると非連続となり，最終的に毛細血管レベルで消失する．かくして，このlayerが脳実質と動脈の間（血管周囲腔）に規則的な境を形成するのである．動脈系では血管周囲腔と脳脊髄液は直接接しない．しかし，血管が軟膜を穿通する際に破綻部が観察され，それを通して脳脊髄液がくも膜下腔と血管周囲腔を行き来するとしている[28,41]．一方，静脈にはこのような構築をなす軟膜からのlayerはなく，静脈と血管周囲腔は直接接している（Fig. 2）．

生理学的には実験的に注入されたトレーサーは，脳実質内とくも膜下腔の間を血管周囲腔に沿い双方向性に移動する[4,9,31]．Rennelsらは動物実験から血管周囲腔を静脈性，動脈性に分けた．血管周囲腔内の内容液は，動脈系では脳実質内へ，静脈系ではくも膜下腔の方向であり，動脈系ではその拍動が内容液の移動に大きな役割を果たすとしている[31]．

このように，脳内血管周囲腔の解剖と生理が動脈と静脈で違いがあることは臨床的に大きな意義をもつ．1例を挙げると，血管周囲腔の拡大は通常高齢者にみられ，小児では稀であることから，脳実質内での動脈の加齢とともに蛇行し，この拍動で，周囲脳が穿たれるとされている[16,28]（Fig. 3）．以上のように，血管周囲腔にまつわる種々の病態を動脈性，静脈性に分けて説明することで，理解しやすくなる．

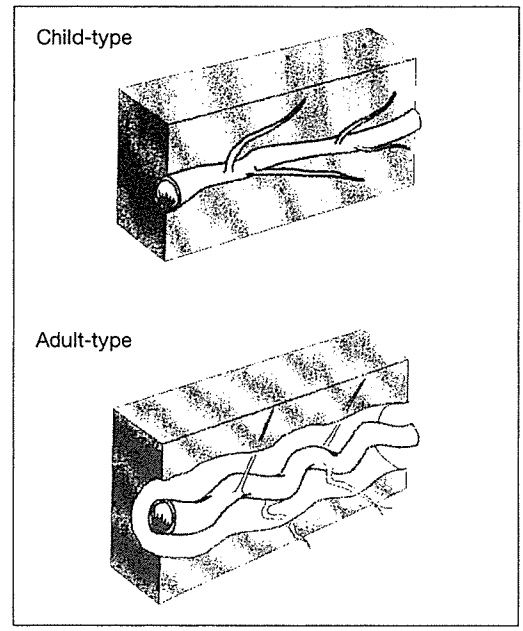

Fig. 3 Diagram illustrating the changes of intracerebral arteies that bring about the condition of perivascular cavities-elongation, dilatation and spiraling of the artery with distortion of branches and separation from brain tissue (from reference 16).

III．脳脊髄液腔描出のためのMRシーケンス

1998年，Matataらは脳槽内の微細な観察に適した撮像法としてheavily T2 weighted MR imagingを紹介した[19]．Saekiらはこのシーケンスが脳実質内の脳脊髄液信号域の局在を鋭敏に反映することを観察した[35-37]．ここでは，Mamata, Saekiらの使用したMRシーケンスで，TR/TE/Excitation：5800/200/4-6.，スライス厚は3 mmで白黒反転像を使用している．

IV．脳内のう胞性疾患との鑑別

日常の脳MR像を観察していると，脳実質内に脳脊髄液に類似した信号域を有するのう胞性疾患に遭遇する．この中に脳内血管周囲腔が拡大した症例があり，画像上脳実質内の占拠性病変との鑑別を要する場合があることが，最近しばしば指摘

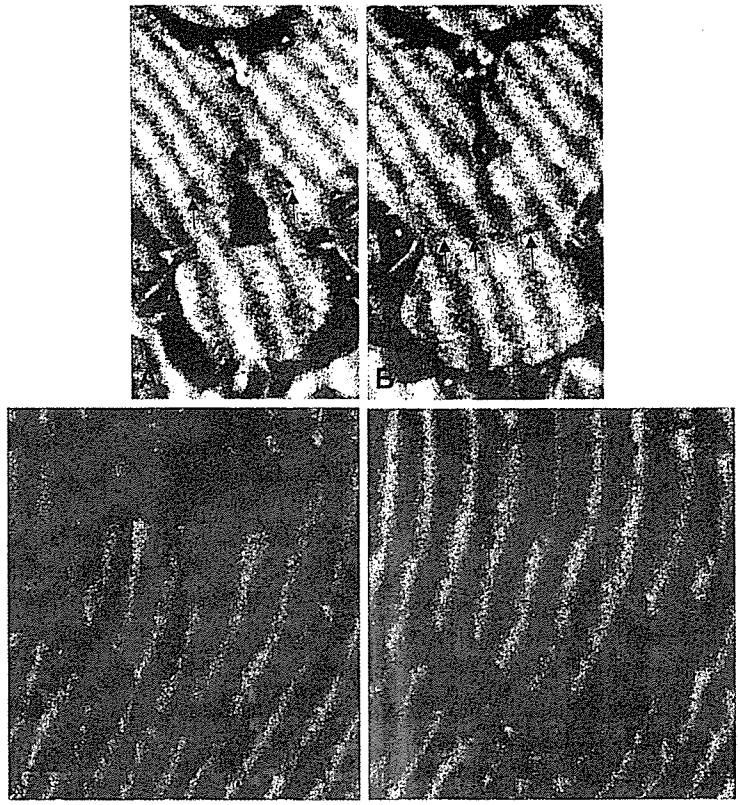

Fig. 4 Heavily T2 weighted MR images of a 19-year-old female. **A** : Coronal section at the cerebral peduncle. Round and ovoid perivascular spaces (**arrows**) are visible at the level of the upper midbrain. **B** : Coronal section 6 mm posterior to Fig. 4A. Small perivascular spaces (**arrows**) are visible at the pontomesencephalic junction and at the level of tentorial margin. **C** : Axial section at the lower midbrain. Ovoid and linear perivascular spaces are visible between the cerebral peduncle and substantia nigra and in the cerebral peduncle. **D** : Axial section 2 slices rostral to Fig 4C. Small perivascular spaces (**arrows**) are visible behind the cerebral peduncle.

されている．また，文献上は，それが臨床症状を呈することが報告され，部位としては，以下に述べるごとく中脳と大脳半球に集中している．

1991年，Elsterらは正常例の20％において，中脳橋移行部で血管周囲腔を確認した．臨床的には，ラクナ梗塞との鑑別疾患として重要であることを指摘した[8]．2005年，Saekiらは脳脊髄液の存在部位をより敏感に反映するheavily T2 weighted imagingを駆使して正常例を観察し，中脳部血管周囲腔は本シーケンスでより高頻度に観察されたと報告した[37]（**Fig. 4**）．その大きさには個人差が大きく，大きいものでは左右径が5 mmに達する例もある（**Fig. 5**）．部位としては，中脳部の上端（間脳移行部）に63%，下端（橋移行部）に87%の例で観察され，水平断でその底部・被蓋部に複数みられた（**Fig. 6**）．前者は後有孔質を穿通し，脳底動脈遠位部や後大脳動脈近位部より分岐するposterior thalamoperforating arteryにより穿通される．後者は，脳底動脈遠位部，上小脳動脈，後大脳動脈近位部より分岐するshort circumferential arteryで，主に大脳脚を穿通する枝が関与する[33]．従来，血管周囲腔がよく観察される部位として，大脳基底核部，大脳皮質などが挙げられるが，Saekiらは中脳部もその1つとし

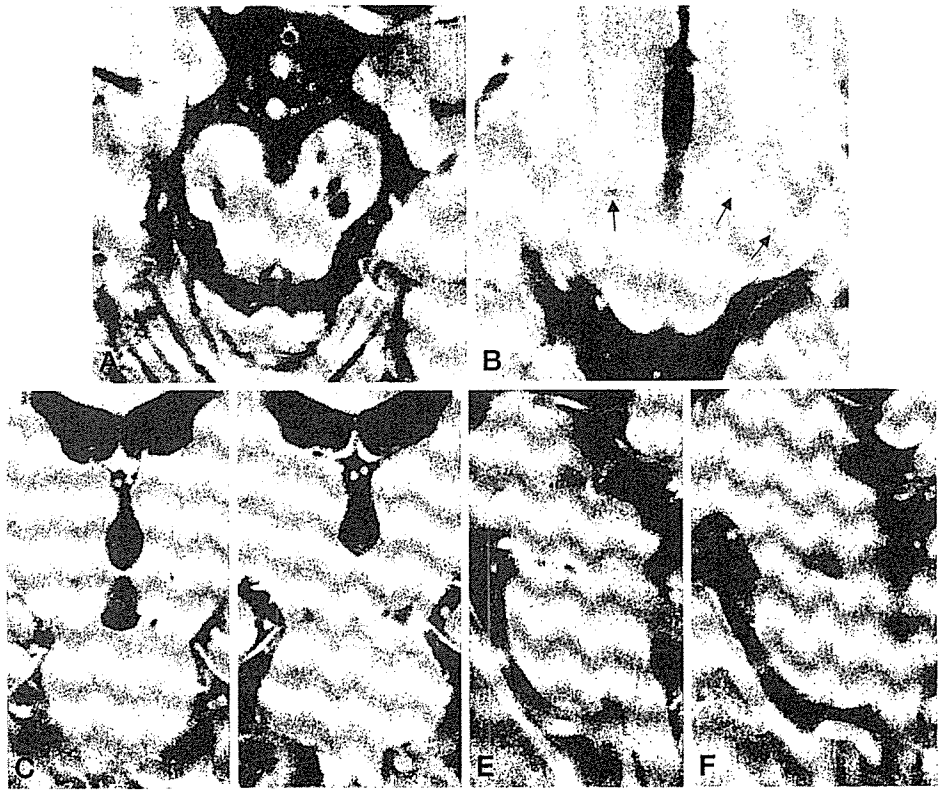

Fig. 5 A 48-year-old male. **A** : Axial section at the lower midbrain. Multiple ovoid and round perivascular spaces are visible between the cerebral peduncle and substantia nigra and in the cerebral peduncle. **B** : Axial section 2 slices rostral to Fig. 5A. Small perivascular spaces (**arrows**) are visible behind the cerebral peduncle. **C** : Coronal section at the anterior midbrain. Dilated perivascular spaces are visible as round or ovoid low signal intensity lesions at the pontomesencephalic and the mesencephalo-diencephalic junctions. **D** : Coronal section at the cerebral peduncle. Dilated perivascular spaces are visible at the level of the pontomesencephalic junction, corresponding to the tentorial margin. The largest of the perivascular space is 5 mm in size. **E** : Sagittal section 6 mm lateral to the midline. Dilated perivascular spaces are visible between the pons and midbrain. **F** : Axial section 12 mm lateral to the midline. Large and small perivascular spaces are visible at the ponto-mesencephalic and mesencephalo-diencephalic juntions.

て明記すべきであることを指摘した[37]．

一方，文献上，剖検と手術例で中脳間脳移行部に髄液信号域の多房性のう胞性病変（multi-lobular cystic lesion）で，中脳水道狭窄や局所症状を呈し，病理や画像所見より血管周囲腔由来の疾患群の報告がある[14, 20, 21, 27, 30, 32, 40]（**Fig. 7**）．現在まで7例が報告されている．臨床症状として，中脳水道狭窄による水頭症6例，片麻痺などの長索徴候やパーキンソン症候群各1例などがある．Poirierらの報告のうち1例では剖検が行われ，病理学的に血管周囲腔の拡大と壊死性血管炎が証明された[30]．後者により血管透過性が増したことが原因であろうと推察している．Saekiらはその文献の中で，他の6例でも同部に生理的に存在する血管周囲腔に何らかの病的修飾が加わり，症状を呈するに至ると考察している[37]．今後，脳幹部でのう胞成分を有する占拠性病変において，gliomaに加えて，その鑑別疾患として，拡大した血管周囲腔（expanding lacunae）の可能性を念頭に置くべきであろう[13,21]．臨床経過については，不明な点が多く，さらなる症例の蓄積を要するが，無症状であれば画像による経過観察でよい

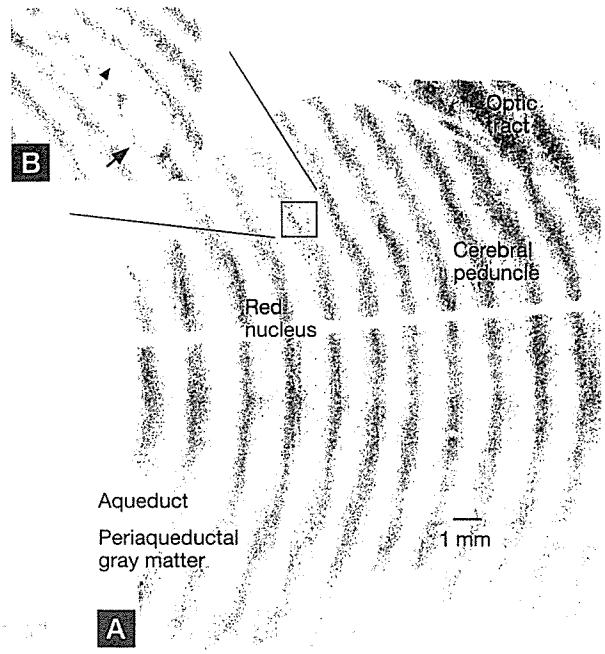

Fig. 6 A : Axial section of the right upper midbrain. Kluver-Barrera stain X 4. Section line between ventral and dorsal halves is noted in the center. Aqueduct, peri-aqueductal gray matter, red nucleus, cerebral peduncle and optic tract are demonstrated. Behind the cerebral peduncle, there is an ovoid space. **B** : Magnified axial section demonstrating the perivascular space at the upper midbrain. H and E stain (original) X 50. The ovoid space includes a vessel (**arrow**) and is lined by pial layer (**arrow head**). No necrotic or ischemic changes were visible in the surrounding brain tissue in this magnified view. These findings histologically suggest that it is a perivascular space.

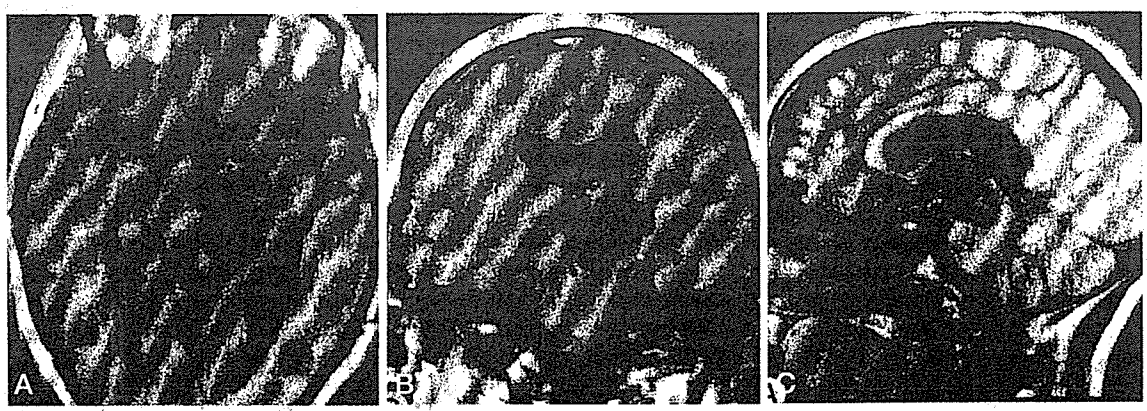

Fig. 7 reference from 39 (reproduced with permission). T1 weighted axial (**A**), coronal (**B**) and sagittal (**C**) images, revealing multilobular CSF-filled expanding spaces at the mesencephalo-diencephalic junction. A 32-year-old female presented with headache and progressive right hemiparesis and MR images revealed multilobular CSF-filled expanding spaces at the mesencephalo-diencephalic junction with ventricular dilatation. She underwent endoscopic fenestration of cyst wall and became free of the neurological deficits.

と考えられる．

1995年，Ogawaらは大脳半球内に多発性の脳脊髄液の信号域を有するのう胞性病変の2例を報告した[25]．1例は後頭蓋窩病変の手術とともに生検を受けた．そして，その病変が拡大した血管周囲腔であることを病理学的に確認した．画像上，脳実質内に髄液信号域を有し，多発性ののう胞をもち（大きいものでは2 cmに達する），軽度の圧迫所見を呈しうる．その後，Komiyamaら，Ohtaら，Saekiらも同様の画像所見を有する症例を報告した[17,26,34]（**Fig. 8, 9**）．しかし，これらの症例ではこの病変による神経症状ははっきりしない．Davisらは一過性の片麻痺を来した症例を報告した．手術を行い，組織診断を得ているが，症

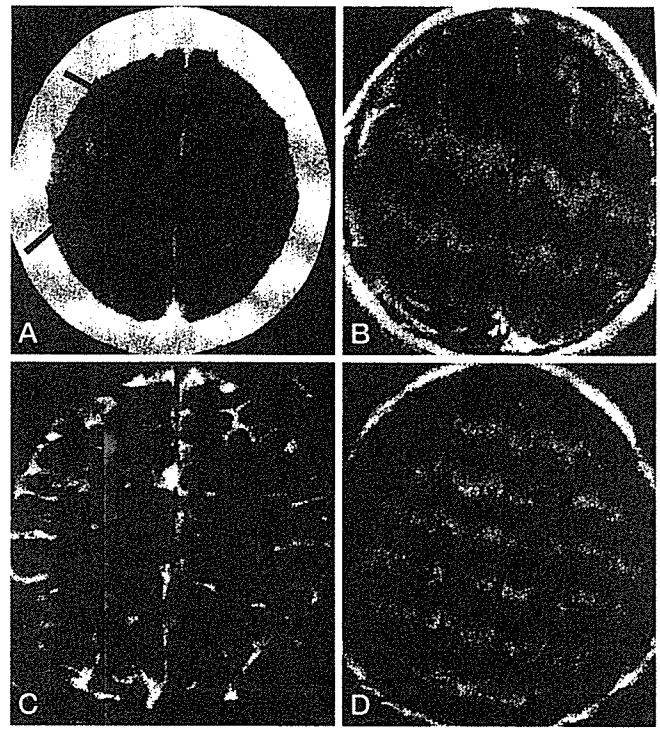

Fig. 8 **A** : CT scan with enhancement. The CT scan showed right hemispheric low density (**arrows**) without enhancement effect. **B** : T1 weighted MR images with contrast medium. The MR image showed irregular low intensity lesion mimicking the brain edema without enhancement effect (**arrows**). The lesion was predominantly limited to one hemisphere. There was a subtle mass effect based on the radiological appearance of the medial margin of the right hemisphere over the midline and less prominent cortical sulci on the right hemisphere. **C and D** : T2 and proton density weighted MR images, respectively. The signal intensity of the lesion (**arrow**) was CSF compatible in both MR sequences. Intraparechymal space occupying lesion such as a glioma in the cerebral hemisphere was suspected.

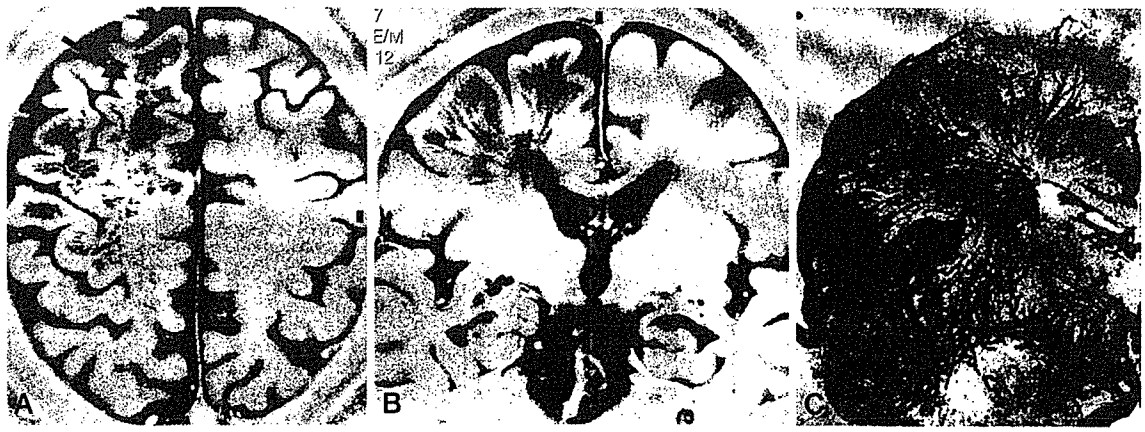

Fig. 9 **A and B** : Heavily T2 weighted (black and white) inverted axial and coronal MR images. The lesions consisted of two components; linear or small oval CSF signal intensity (**arrow**) and surrounding edema-like changes, which seemed to be located in the white matter. The linear and small ovoid parts conformed to the pathways of the medullary arteries (Fig. 9C). This strongly supports that the low signal intensities are related to the perivascular spaces. **C** : Microangiography of cerebral hemisphere from reference 38. Medullary arteries, conforming to the low signal intensity in the cerebral cortex in Fig. 9B, are clearly shown.

候性か無症候性かは不明である[6]．臨床上，脳実質内の病変，neuroepithelial tumor, ganglioglioma, encysted encephalomalacia, 炎症性あるいは感染性のう胞性疾患，そして，glioma との鑑別が問題となる[6,17,26,34,42]．筆者らは，脳ドックなどで大脳半球部を注意深く観察していると，偶発的に大脳半球に拡大した血管周囲腔に合致した所見を有する症例に遭遇した（**Fig. 10**）．これらのことを

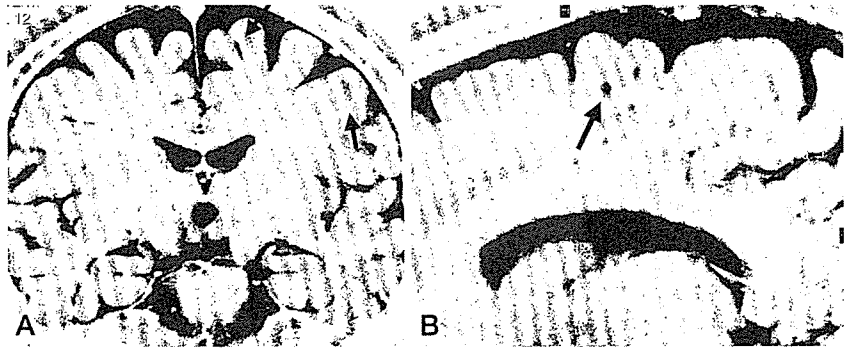

Fig. 10 Relatively marked perivascular spaces are incidentally noted in a patients with chronic tension headache.

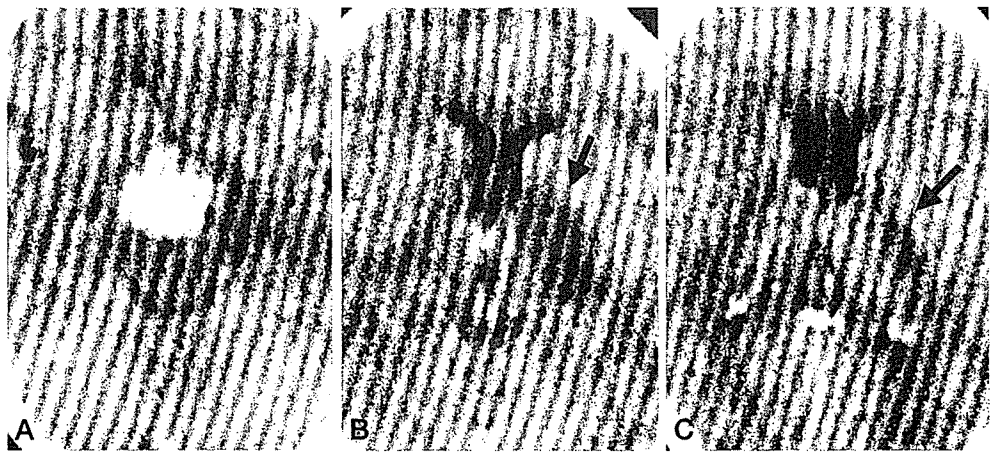

Fig. 11 CT scans of a 33-year-old female with craniopharyngioma. **A** : High density lesion was seen in the pituitary region. **B and C** : The low density lesion was found in the brain along the internal capsule. The ischemic change was suspected along the territory of the anterior choroidal artery.

考え合わせると，MRシーケンスで大脳半球内の占拠性病変でのう胞内容が脳脊髄液に一致する場合は拡大した血管周囲腔を疑う必要がある．多くの例で年単位の観察後にも変化がみられていない．本疾患を疑う場合，基本的に経過観察でよいと考えられる．

このように，脳実質内ののう胞性病変の中に，血管周囲腔の拡大した症例が混在している可能性がある．良好な自然経過をたどる例が多く，その治療選択には慎重でなければならない．

V．視索沿いの浮腫様変化

従来，頭蓋咽頭腫例の画像を観察していると，付随した症状に乏しいものの術前後に内包付近の前脈絡叢動脈領域に梗塞様の変化をみることがある（**Fig. 11**）．これは視索に沿った浮腫様変化として報告されている．視索上部と付近の視床下部，内包，著明な例では大脳基底核に及ぶ[12,24,43]．この浮腫様変化は頭蓋咽頭腫に特異的な所見として報告され，その診断に有用であるとされてきた．その発生機序として，炎症性変化を喚起しやすいのう胞内容液が視索とその周辺に vasogenic edema を起こすためとされてきた[24]．しかし Saeki らは，50 例の下垂体部腫瘍の治療前後の画像所見を比較し，浮腫様変化は頭蓋咽頭腫に特異的な所見ではなく，悪性リンパ腫，胚細胞腫，転移性